

2-23-2026

Preparation, Characterization, and Antimicrobial Evaluation of a Cefepime Derivative with Divalent Transition Metals

Zahraa A. Jaber

Department of Chemistry, College of Science for Women, University of Baghdad, Baghdad, Iraq,
zahraaj_chem@csu.uobaghdad.edu.iq

Israa H. Ibraheem

Department of Chemistry, College of Science for Women, University of Baghdad, Baghdad, Iraq,
israahi@csu.uobaghdad.edu.iq

Sahar S. Hassan

Department of Chemistry, College of Science for Women, University of Baghdad, Baghdad, Iraq,
saharsh_chem@csu.uobaghdad.edu.iq

Follow this and additional works at: <https://bsj.uobaghdad.edu.iq/home>

How to Cite this Article

Jaber, Zahraa A.; Ibraheem, Israa H.; and Hassan, Sahar S. (2026) "Preparation, Characterization, and Antimicrobial Evaluation of a Cefepime Derivative with Divalent Transition Metals," *Baghdad Science Journal*: Vol. 23: Iss. 2, Article 3.

DOI: <https://doi.org/10.21123/2411-7986.5195>

This Article is brought to you for free and open access by Baghdad Science Journal. It has been accepted for inclusion in Baghdad Science Journal by an authorized editor of Baghdad Science Journal.



RESEARCH ARTICLE

Preparation, Characterization, and Antimicrobial Evaluation of a Cefepime Derivative with Divalent Transition Metals

Zahraa A. Jaber[✉]*, Israa H. Ibraheem[✉], Sahar S. Hassan[✉]

Department of Chemistry, College of Science for Women, University of Baghdad, Baghdad, Iraq

ABSTRACT

The Schiff base ligand (L)- 1-((7-((Z), was recently synthesized 2-(2-((Z)-5,5-diethyl2-(methoxyimino)acetamido)-2-(methoxycarbonyl)-2,6-dioxotetrahydropyrimidin-4(1H)-ylideneamino) thiazol-4-yl8-oxo-5-thia , the next mineral ions, Ni²⁺, Cu²⁺, Zn²⁺, and Co²⁺, are permitted to react with 1-azabicyclo[4.2.0]oct-2-en-3-yl)methyl)-1-methylpyrrolidinium, leading to the formation of new metal complexes with distinct geometric shapes. By detecting the shifting in the azomethines band and the appearance of M-N and M-O bands, FT-IR confirmed the occurrence of coordination through N of azobenzene and two O atoms of beta lactam and ester, indicating the development of Schiff base complexes as well as the original Schiff base. Additionally, we can use such equipment to find out if there are any aquatic water molecules inside the coordination sphere. By observing the shifting of electronic transitions that occurred in the ligand at the ultra violet region, the UV-Vis spectra of all the resultants demonstrated the formation of coordination. TGA analysis of the ligand. Furthermore, the results of the FAA and molar accessibility were more in line with the counting results. The diagnosis revealed trientate dental behavior, tetrahedral geometry for the cobalt complex, and octahedral geometry for the remaining complexes, along with mononuclear complexes. As described in the publication, we have evaluated the antibacterial property of Schiff base and its complexes on a variety of microbes.

Keywords: Barbiton, Biological activity, Cefepime, MetalComplexes, Schiff base, Thermogravimetric analysis**Introduction**

Hugo Schiff discovered the Schiff Base after he found out about the reversible acid-catalyzed condensation process containing primary amine plus carbonyl compounds.¹ Researchers are interested in the chemistry of metal complexes caused by Schiff Base ligands that contain nitrogen and oxygen, such as donor atoms. It is known that ligands can interact with metal atoms in a variety of ways depending on the circumstances of the reaction. The condensation reaction between primary amines and aldehydes produces ligands. The biological activity of Numerous Schiff base metal complexes has a range of medicinal uses. For instance, the biological features of transi-

tion metal complexes of Schiff Base ligands having “N” and “O” donor atoms, such as their antibacterial, anti-inflammatory, antioxidant, antitubercular, anti-convulsant, antifungal analgesic, and anthelmintic effects, make them highly focused.²

The activity technique’s key characteristic is the core metal ion. Coordination agents like Schiff bases can be used to combat a range of medical issues associated with toxicity from free metal ions.³ Moreover, the quantity, kind, and proportionate location of the ligand donor atoms allow a strong control over the stereochemistry of the metallic, contributing to the number of ions in hetero and homo-polynuclear complexes.⁴ Schiff bases are superior candidates for the preparation of metal complexes of interest in

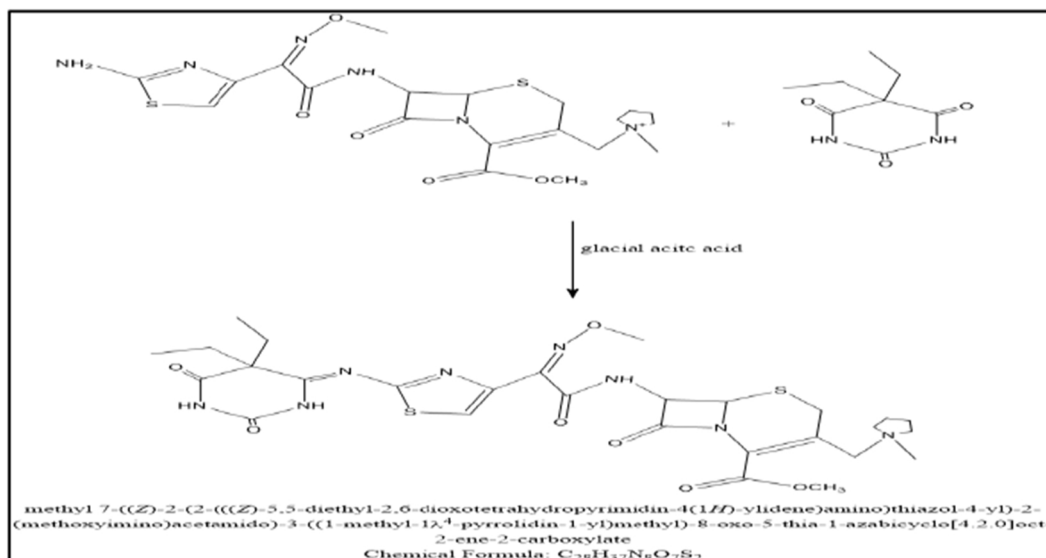
Received 11 April 2024; revised 29 December 2024; accepted 31 December 2024.
Available online 23 February 2026

* Corresponding author.

E-mail addresses: zahraaj_chem@cs.w.uobaghdad.edu.iq (Z. A. Jaber), israahi@cs.w.uobaghdad.edu.iq (I. H. Ibraheem), saharsh_chem@cs.w.uobaghdad.edu.iq (S. S. Hassan).

<https://doi.org/10.21123/2411-7986.5195>

2411-7986/© 2026 The Author(s). Published by College of Science for Women, University of Baghdad. This is an open-access article distributed under the terms of the Creative Commons Attribution 4.0 International License, which permits unrestricted use, distribution, and reproduction in any medium, provided the original work is properly cited.



Scheme 1. Preparation of ligand (L).

Table 1. Physical -properties element microanalysis studies of ligand and complexes.

Compounds	Found Elemental Analysis(cal.)						M.P°C	Color	%Yield	$\mu_s \text{ cm}^{-1}$
	C	H	N	O	M	S				
C ₂₇ H ₃₇ N ₈ O ₆ S ₂ (L)	(50.71) 50.82	(5.31) 5.64	(15.96) 16.93	(16.01) 16.92	—	(8.97) 9.69	230–231	Dark yellow	87%	—
C ₂₇ H ₃₇ CoN ₈ O ₆ S ₂ (Co L)	(46.02) 46.82	(5.11) 5.38	(17.09) 16.18	(13.12) 13.86	(79.5)1 8.50	(9.88) 9.26	240–242	Blue	63%	14.00
C ₂₇ H ₄₁ NiN ₈ O ₈ S ₂ (Ni L)	(43.93) 43.16	(15.21) 15.50	(13.42) 13.89	(17.19) 17.84	(7.04) 7.27	(7.34) 7.95	250–251	Light green	83%	63.03
C ₂₇ H ₄₁ CuN ₈ O ₈ S ₂ (Cu L)	(42.06) 42.90	(5.07) 5.46	(13.23) 13.80	(17.45) 17.74	(7.33) 7.83	(7.51) 7.90	243–245	Dark green	77%	71.66
C ₂₇ H ₄₁ ZnN ₈ O ₈ S ₂ (Zn L)	(42.22) 42.81	(5.12) 5.45	(13.58) 13.77	(17.32) 17.70	(7.94) 8.04	(7.11) 7.88	254–255	Light yellow	89%	78.93

Table 2. FTIR absorption bands of metal complexes.

Comp.	n (NH)	n (C=O)		n (M-N)	
	amid	n (C=N)	β -Lactam	amid	n (M-O)
(L)	3220	1666	1766	1700	—
(Co L)	3243	1669	1770	1718	456
(NiL)	3233	1673	1769	1730	425
(Cu L)	3250	1672	1768	1720	416
(ZnL)	3224	1676	1775	1743	433

bioinorganic chemistry, encapsulation, separation, transport, and catalytic processes because of all these characteristics. This study served as a guide for synthesizing a Cefepime derivative (Cefepime is a fourth-generation cephalosporin antibiotic) with di-valent transition metals, the structures of which were determined by a number of characterization analyses. On the other hand, specific metal complexes demonstrated a strong ability to operate as antifungal, antiviral, anticancer, and unique biological activities, such that the combined effects of multiple therapeutic agents are shown to increase in efficacy.^{5,6} Schiff

Base metal complexes are considered one of the most important fields of research, with the primary goal of discovering effective and safe therapeutic agents for treating cancer and bacterial infections.⁷

Materials and methods

The metal salt provided by Fluka (CoCl₂.6H₂O, NiCl₂.6H₂O, CuCl₂.6H₂O, and ZnCl₂.6H₂O) was used in this study. The Shimadzu 8400 Fourier-Transform-Infrared Spectroscopy was employed to record the

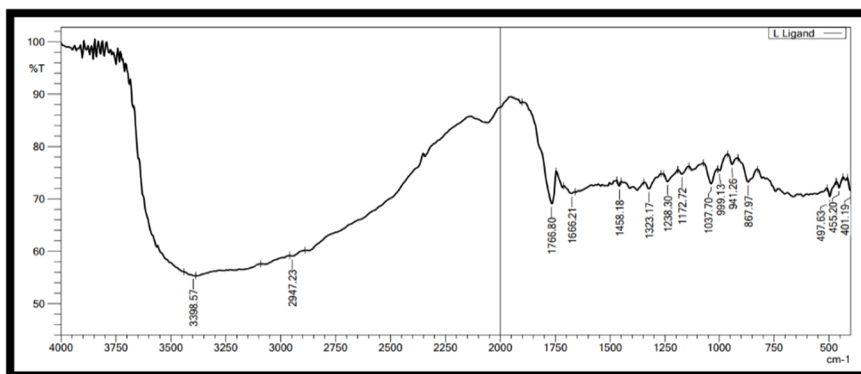


Fig. 1. The FTIR-spectrum of ligand (L).

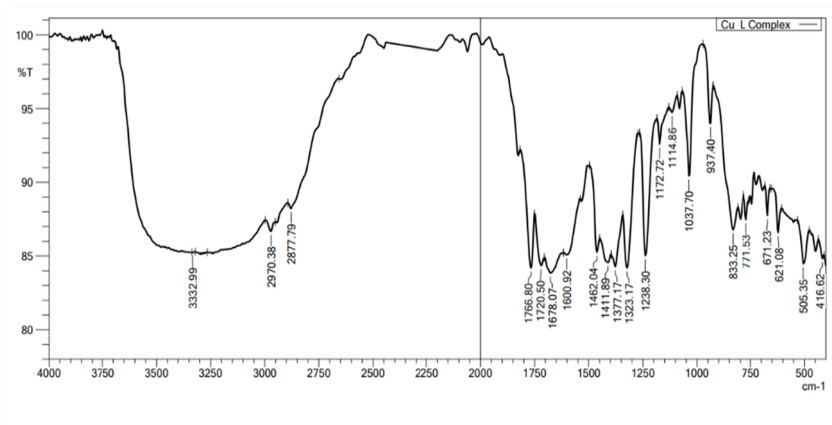


Fig. 2. The FTIR-spectrum copper complex (CuL).

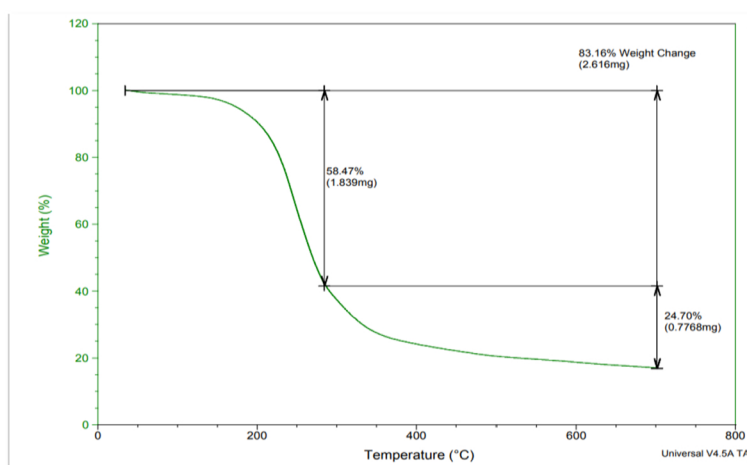


Fig. 3. TGA for ligand (L).

FTIR, with a wavelength range of 4000–200 cm^{-1} and UV-Vis (1600A). The electronic spectra in the wavelength range of 190–1100 nm were recorded using Shimadzu. A Perkin-Elmer 500 Atomic-Absorption - Spectrophotometer was employed for analyzing the

metal. A Conductivity-Meter 220 provided with a Gall encamp was utilized to measure the molar conductivity in ethanol as a solvent at room temperature. B-6000.01 M.F. was employed as a melting tool.

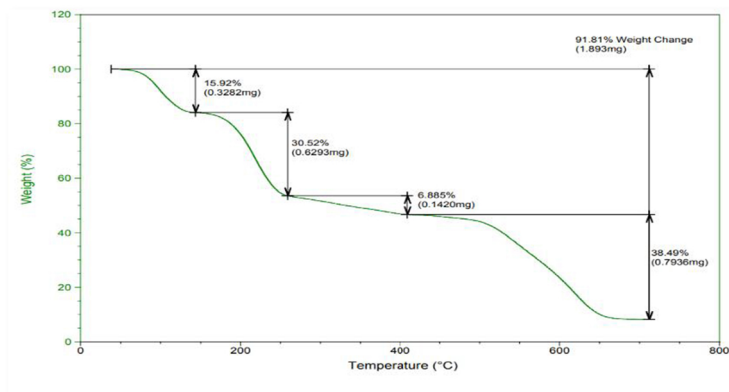
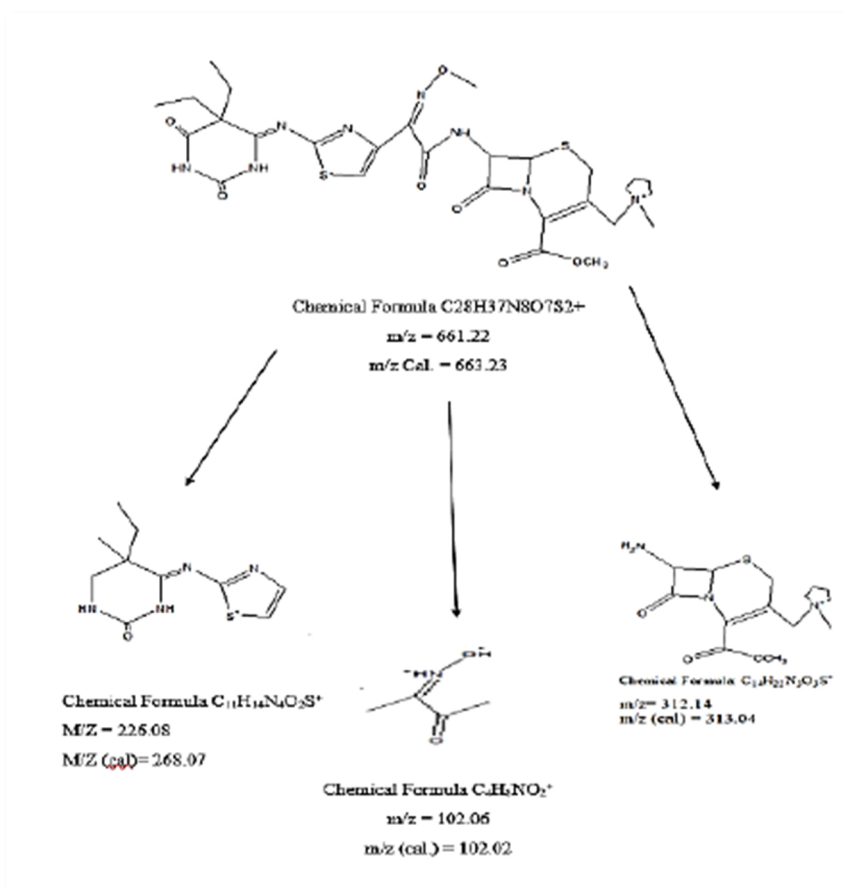


Fig. 4. TGA for copper complex CuL.



Scheme 2. The mass fragmentation pattern of ligand (L).

Preparation of Ligand (L): A mixture of barbitone (0.184g, 0.524 m. mole) and (0.553 g, 0.533m.mole) of cefepime dissolved in hot ethanol (20 ml), then 2ml of glacial acetic acid was added. The reaction mixture was heated below refluxing for six hours at 60°C with unceasing stirring. A yellow precipitate was formed, and the solution color was changed to dark yellow. TLC monitored the progress of the reaction.

The product was filtered afterward and then washed by a hot mix of methanol: water (v:v) (80:20) % and recrystallized from ethanol, [Scheme 1](#).⁸

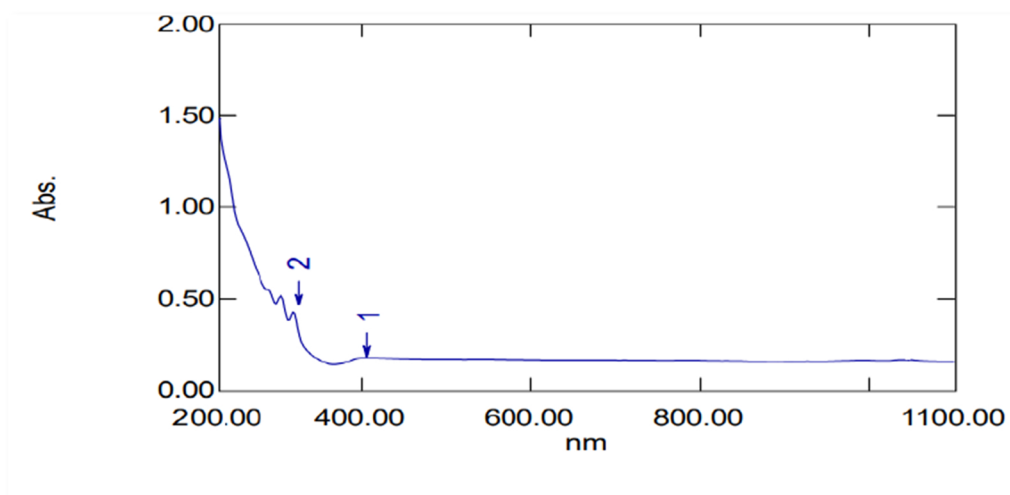
Preparation of Complexes: To prepare novel metal complexes, a general procedure was followed: (0.237, 0.237, 0.17, 0.136 g, 1 m mole) of hydrate metal salts of cobalt, nickel, copper, and zinc dissolved in 10 ml of 100% ethanol was reacted with,

Table 3. The mass loss percentage of ligands and their complexes for TGA.

Comp.	No. Steps	Estimated mass loss (Cal.)	Remnant mass loss (Cal.)
(L)	2	83.17 (83.16)	16.83 CU(16.81)
(Co L)	3	87.52 (87.94)	12.48 (12.06)
(Ni L)	4	80.74 (80.89)	19.26 (19.11)
(Cu L)	4	91.81 (91.95)	8.19 (8.05)
(Zn L)	4	85.32 (85.85)	14.68 (14.15)

Table 4. The electronic absorption of ligands and their complexes.

Comp	λ nm	Absorption Bands cm^{-1}	Assignment
L	340	29411	$\pi-\pi^*$ (C=C)
	230	43478	$n-\pi^*$ (CO, CN)
	221	45488	
Co L		3370 from FTIR	$^4T_{1g} \rightarrow ^4T_{2g}$
	770	5288 (cal.)	$^4T_{1g} \rightarrow ^4T_{1g}$
	380	12987	$^4T_{1g} \rightarrow ^4A_{2g}$
	351	26315	I.L
		28490	I.L
Ni L	892	11211	$^3A_{2g} \rightarrow ^3T_{2g}$
	635	15748	$^3A_{2g} \rightarrow ^3T_{1g(F)}$
	480	20833	$^3A_{2g} \rightarrow ^3T_{1g(P)}$
	277	36101	I.L
Cu L	820	12195	$^2E_g \rightarrow ^2T_{2g}$
	378	26455	Charge Transfer
	220	45454	I.L
Zn L	368	27173	I.L
	228	43859	C.T

**Fig. 5.** The electronic-spectrum of ligand (L).

and (0.73 g. 1 m mole) of ligand was mixed within the same solvent. At room temperature, the reaction mixture was refluxed for three hours at 60°C. TLC

monitored the progress of the reaction. The product was filtered afterward, then washed with water and recrystallized from ethanol.⁹

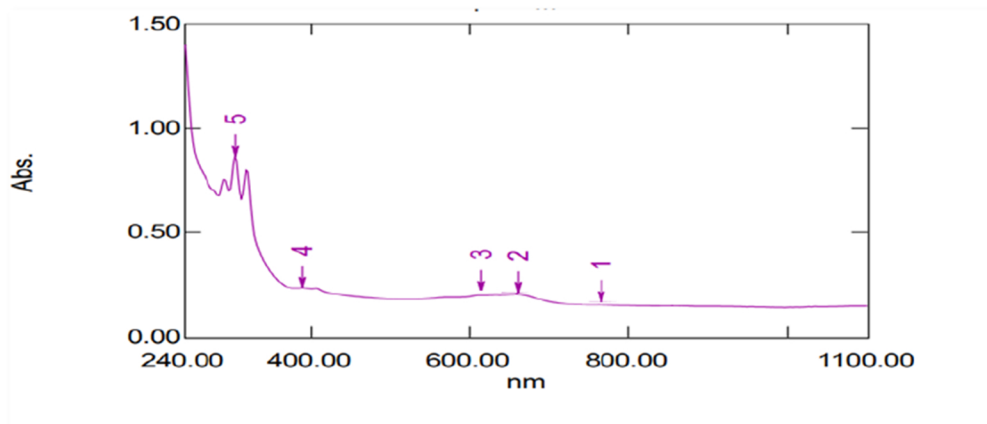


Fig. 6. The electronic spectrum of cobalt complex (Co L).

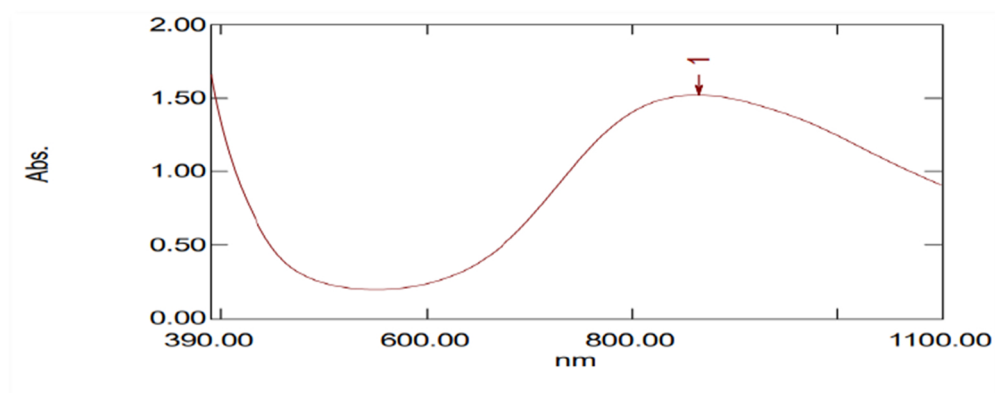


Fig. 7. The electronics spectrum of the capper complex (Cu L).

Table 5. The ¹HNMR shifts.

No. of Protons	S (ppm)
s(3H-CH ₃)	1.95
DMSO	2.49
s(3H-OCH ₃)	2.55
s(4H - CH ₂)	3.07
s(5H- β- lactam)	3.71
s(8H- C ₄ H ₈ Cyclo)	3.81
s(3H - NH)	7.23
s(8H- Barbiton)	7.62
s(3H-N-O-CH ₃)	8.82

Table 6. The ¹³CNMR shifts of ligand.

No. of Carbon	S (ppm)
m(DMSO)	39.06-40.73
m 4(C ₄ H ₈)	9.64
s2(COCH ₃)	21.82
s2(CH ₂)	23.63
s6(β-lactam)	31.65
s6(Barbiton)	55.16
s3(C=N)	56.89
s2(C=S)	150.38
s2(C-NH)	173.51

Results and discussion

The complexes were stable at room temperature as colored powders. Table 1 summarizes their physico-chemical characteristics based on the analytical data, a molar ratio of 1:1 (M: L) for all produced complexes.

FT-IR analysis

FTIR spectroscopy for the ligands and their complexes were investigated, verified, and compared to values reported in the literature.^{10,11} The creation of Schiff's base was confirmed by the C=N stretching band, which caused several notable ligand absorption bands at 1666 cm⁻¹. In addition, the ligand contains essential aggregates such as the C=O band in β-Lactam group,^{12,13} where the absorption packets for these groups in the free ligand were diagnosed with the following- The result of these packages in terms of location, severity, and shape when coupled with metal ions where the ligand showed absorption packages C=O band for amide & β-lactam 1700 and 1766

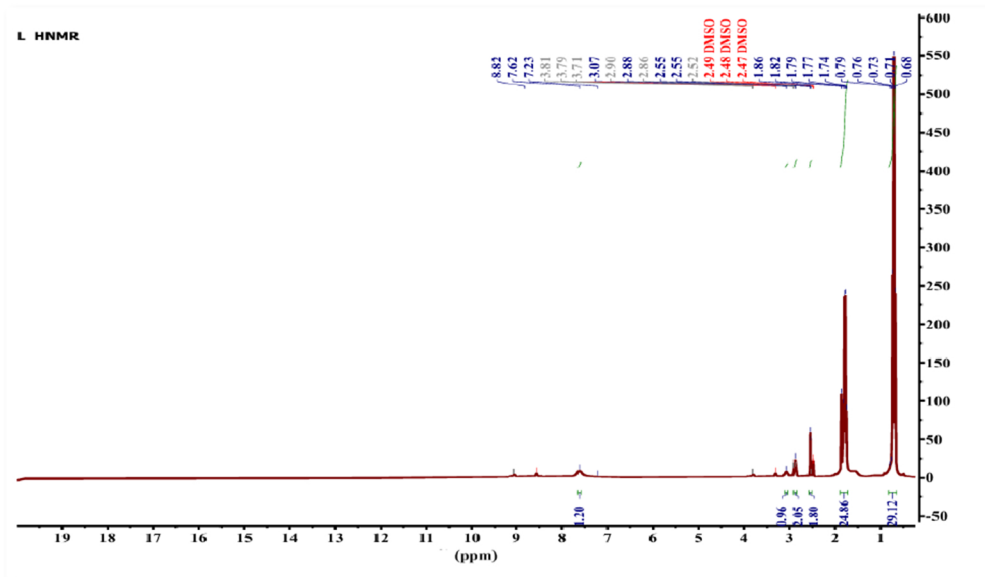


Fig. 8. The ^1H NMR Spectra of ligand (L).

cm^{-1} respectively. The C=N stretching band of Liang was shifted to a higher-wave number in the range of 3–10 cm^{-1} as a result of the ligand complexing with metal.¹ Additionally, for the all-metal coordination, the absorption band at 3220 cm^{-1} corresponding to the NH stretching of the ligand was moved to the 4–30 cm^{-1} range. The M–N system is responsible for the emergence of a new absorption band below 500 cm^{-1} .^{14,15} Linkage in the range of 505–520 cm^{-1} due to M–O coordination. A compound can be formed by ligands complexing with metals in all absorption bands. Table 2 and Figs. 1 and 2 illustrate the main FTIR absorption bands.

TGA

The results of thermal analysis for ligands and their synthesized complexes are exhibited in Figs. 3 and 4, respectively. Scheme 2 provides an overview of the metal complexes' preliminary decomposition reaction. Based on the thermograms, stages of decomposition, the decomposition products' temperature ranges, and weight-loss complex percentages, they were determined. There was an agreement of estimated values and thermal decomposition results, proving the elemental analysis results. It was noticed that carbon remained in the ligand, while the remaining metal oxide was in the ligand and metal complexes of Co, Ni, Cu, and Zn. The ligand decomposes and the complexes in 2–4 phases according to the results of the thermogravimetric tests,¹⁶ The technique proves that the ligand (L) was analyzed in two steps. Fig. 3 shows the mass loss percentage; it was

revealed that the estimated mass loss was 83.17%, and the remnant was 16.83%, where the calculated mass loss was 83.16%, and the remnant was 16.84%. The mass loss of all complexes is illustrated in Table 3.

Electronic spectrum

Using the information in the Tanabe-Sugano diagram, the electronic absorption spectrum was applied to forecast the geometry based on the quantity and shape of observed peaks plus those calculated once.

The electronic-spectrum of the L, Fig. 5, displays three key bands. The π - π^* transitions in the (C=C) group were responsible for the primary absorption bands at 29411 cm^{-1} . The absorptions 2 and 3 occurred at 43478, and 45488 cm^{-1} and were ascribed to n - π^* . These groups might be situated in the (C=O, C=N, CS, and NH) groups⁹.

Co L complex's UV-vis spectra showed a band at 12987 cm^{-1} in the present research, to $^4\text{A}_2 \rightarrow ^4\text{T}_1(\text{p})$. Since the $^4\text{A}_2 \rightarrow ^4\text{T}_2$ and ν_2 $^4\text{A}_2 \rightarrow ^4\text{T}_1$ transitions are out of the UV device's scale, they do not show up in the spectrum. The IR spectrum is used to compute these transitions. The measured value was 3370 cm^{-1} . Using the Tanabe-Sugano diagram for the d^7 system, the second transition was theoretically computed from Eq. 15B = $\nu_3 + \nu_2 - 3\nu_1$. A transition was observed at 5288 cm^{-1} . NiL complex has four bands (11211, 15748, and 20833) cm^{-1} . CuL¹⁰ complex displayed three-bands in wave-number (12195, 26455, and 45454) cm^{-1} . ZnL complex^{17,18} exhibited two bands in the wave number of 27173, and 43859

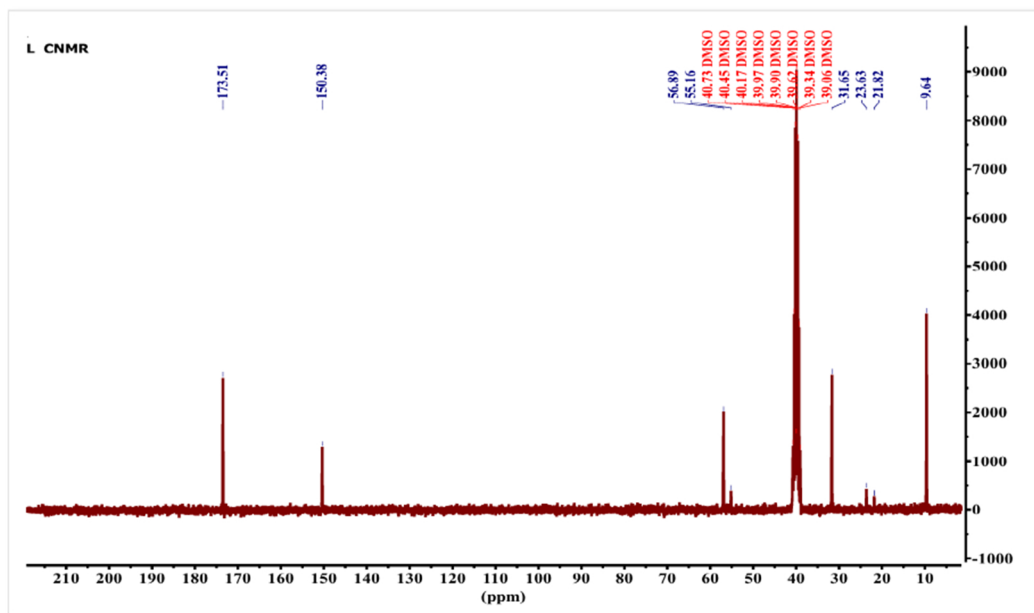


Fig. 9. The ^{13}C NMR shifts the spectrum of ligand.

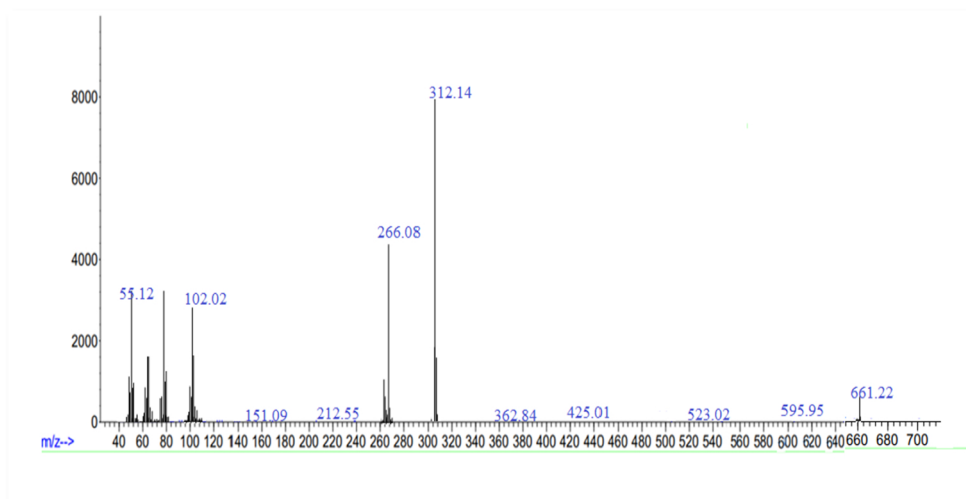


Fig. 10. The mass-spectrum of ligand (L).

Table 7. The effect of ligand and its metal complex on staphylococcus aureus, escherichia coli, and candida albicans. c in 5 mM.

Comp.	<i>Staphylococcus aureus</i>	<i>Escherichia Coli</i>	<i>Candida albicans</i>
	5Mm	5mM	5Mm
CoL	20	22	18
NiL	16	24	11
CuL	17	11	9
ZnL	18	20	10
L	18	22	16
EtOH	-	-	-

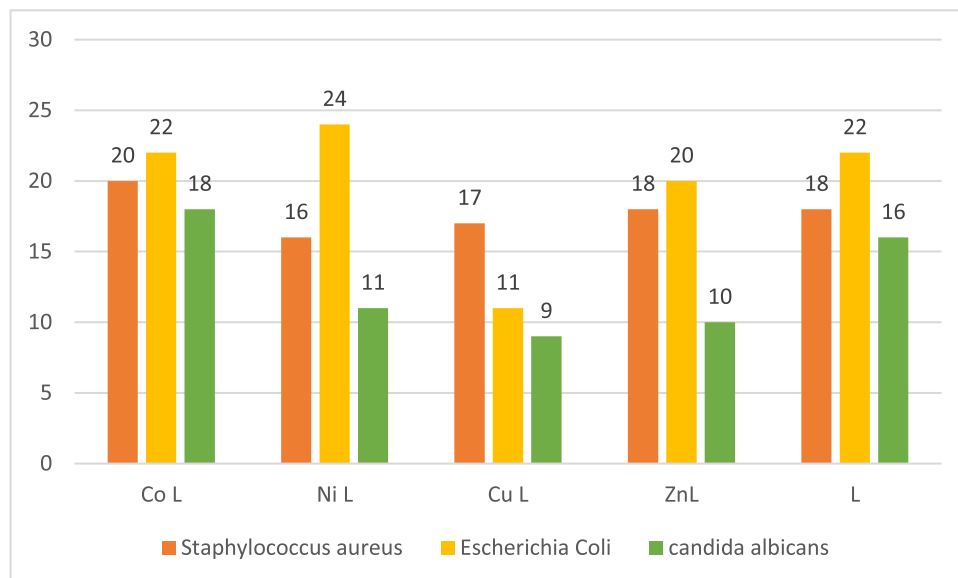


Fig. 11. The effect of prepared compounds on staphylococcus aureus, escherichia coli, and candida albicans in 5 mM.

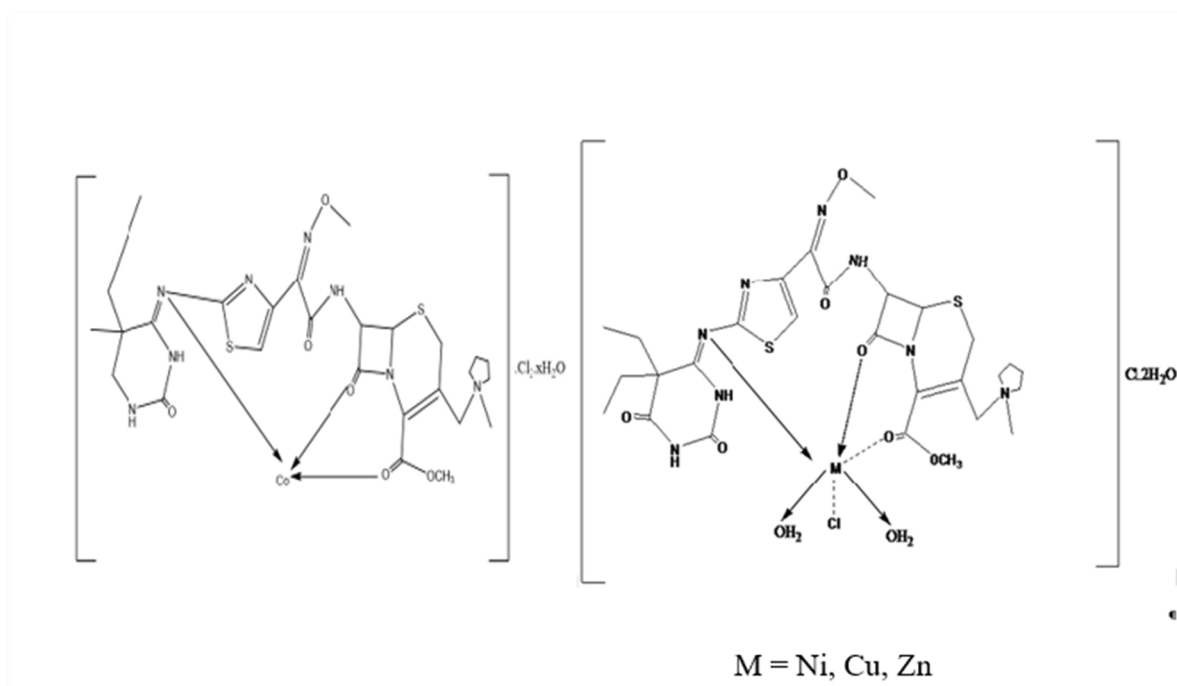


Fig. 12. The suggested structure of the complexes.

cm^{-1} . All transition bonds are illustrated in Table 4 and Figs. 5 to 7.

$^1\text{H-NMR}$ & $^{13}\text{C-NMR}$ Spectrum of ligand

The $^1\text{H-NMR}$ and $^{13}\text{C-NMR}$ spectra¹⁹ of ligand (L), Scheme 1, demonstrate these spectra' chemical shifts. $^1\text{H-NMR}$ (DMSO- d_6 , 2.5 ppm) and others are

illustrated in Table 5 and Figs. 8 and 9 $^{13}\text{C-NMR}$ (DMSO- d_6 30–40) & others in Table 6 and Fig. 9.

Mass spectrum of ligand (L)

The mass spectrum of ligand L was measured using a mass device. This method is crucial for characterization and works in tandem with other methods to determine the compound's molecular weight based

on the relation (m/z)20. Scheme 2 displays the retrieved mass and the fragmentation pattern based on the ligand's mass information. The mass spectrum chart is illustrated in Fig. 10.

The evaluation of antibacterial-activity

The metal complexes of the mixed ligand were tested against the bacteria in order to investigate the in vitro biological screening effects. Nutrient agar was used as the medium, and the disk diffusion technique was used to accomplish this. Using a micropipette, the test solution was added to the well, and the plates were then incubated for 24 hours at 37°C. Using a ruler, the inhibition zone of each pore was measured in millimeters. By evaluating the growth inhibition around the disk, the findings were recorded.²⁰ The theory of Chelation and the overtone concept can be used to explain why the metal complexes possess a higher inhibition zone compared to the ligand. Because of the ligand orbital overlap and partial sharing of the metal's positive charge in the donor groups during chelation, the polarity of the metal ion will be reduced more than it was previously.

In addition, it raises the π -electrons delocalization over the full chelating ring, blocks the metal binding sites in microorganisms' enzymes, and improves complexes' penetration into the lipid membranes. Chelation theory and the overtone idea can explain why the metal complexes have a higher inhibition zone than the ligand.^{21,22} The result is illustrated in Fig. 11 and Table 7.

The suggested structure of synthesized complexes is illustrated in Fig. 12.

Conclusion

This study developed the ligand cefepime derivative and its metal complexes, which were studied by a variety of physicochemical and spectral tests. The results indicated that the produced ligand forms a six-member ring when it is attached to the metal ion in a tridentate via the amide, the nitrogen atom of the azomethane group, and two oxygen atoms of the carbonyl group; thermogravimetric tests also characterized the complexes. The findings regarding antifungal and antibacterial data proved that some metal complexes exhibit more biological activity in comparison to their parent ligand.

Author's declaration

- Conflicts of Interest: None.

- We hereby confirm that all tables and figures belong to us. Besides, figures and images that are not ours were given permission for republication.
- No animal studies are present in the manuscript.
- No human studies are present in the manuscript.
- Ethical Clearance: The project was approved by the local ethical committee at the University of Baghdad.

Author's contribution

S.S.H conceived the research idea, conducted a literature search, and discussed the results in addition to writing the manuscript. Z.A.J carried out the practical part of preparing the raw materials in cooperation with I.H.I All of the authors prepared the complexes, conducted preliminary tests, and participated in editing and approving the last draft of the manuscript.

References

1. More MS, Joshi PG, Mishra YK, Khanna PK. Metal complexes driven from Schiff bases and semicarbazones for biomedical and allied applications. *Mater Today Chem.* 2019;14:100195. <https://doi.org/10.1016/j.mtchem.2019.100195>.
2. Ommenya FK, Nyawade EA, Andala DM, Kinyua J. Synthesis, characterization and antibacterial activity of Schiff base, 4-chloro-2-((e)-[(4-fluorophenyl)imino]methyl}phenol metal (II) complexes. *J chem.* 2020;30:1–8. <http://dx.doi.org/10.1155/2020/1745236>.
3. Mahdi S, Abdul Kareem LK. Synthesis, characterization, anticancer and antimicrobial studies of metal nanoparticles derived from Schi base complexes. *Inorg Chem Commun.* 2024; 165:112524. <https://doi.org/10.1016/j.inoche.2024.112524>.
4. Ibraheem IH, Mubder NS, Abdullah MM, Al-Neshmi H. Synthesis, characterization and bioactivity Study from azo – ligand derived frommethyl-2-amino benzoatewith some metal ions. *Baghdad Sci J.* 2023;20(1):0114–120. <http://dx.doi.org/10.21123/bsj.2022.6584>.
5. Figgis B, Hitchman M. Ligand filed theory and its application. *J Chem Educ.* 2002;79(9):1072. <https://doi.org/10.5860/choice.38-3916>.
6. Dabrowiak JC. *Metals in medicine.* Hoboken: Wiley, 2017. pp. 218. <http://dx.doi.org/10.1002/9781119191377>.
7. Majeed WH, Baqer SR. Preparation of new series of tetradentate schiff base complexes and studing them spectroscopically, biologically and theoretically. *Iraqi J Market Res Consum Prot.* 2023;15(1):106–119. [http://dx.doi.org/10.28936/jmraipc15.1.2023.\(10\)](http://dx.doi.org/10.28936/jmraipc15.1.2023.(10)).
8. Hadi K, Amir AA, Muhammad NT, Muhammad A, Khurram, SM. Synthesis, spectral characterization, crystal structure and antibacterial activity of nickel (II), copper (II) and zinc (II) complexes containing ONNO donor Schi base ligands. *J.Mol Struct.* 2021;1233:130112–130126. <https://doi.org/10.1016/j.molstruc.2021.130112>.
9. Kasim SM, Yassir FA, Hammoodi SH, Mustafa YF. A review of schiff base-inorganic complexes and recent advances in their biomedical and catalytic attributes. *Eurasian Chem Commun.* 2023;5(6):522–535. <https://doi.org/10.22034/ecc.2023.379484.1587>.

10. Abd AL,Qadir NA, Shaalan ND. Synthesis, characterization and biological activity study for some new metals complexes with (3Z,3'E)-3,3'-(((2E,5E)-hexane-2,5-diylidene)bis(hydrazine-2,1-diylidene))bis(indolin-2-one). IHJPAS. 2023;36(3): 231–244. <https://doi.org/10.30526/36.3.3071>.
11. Kareem SH, Hassan SS, Ahmed MF, Ibrahim SK, Alias MF. Synthesis, spectroscopic characterization, and biological evaluation of some transition metal complexes from C16H19N3O3S Ligand. JGPT 2019;(11):198–208.
12. Salih NAM. Synthesis, characterization, and bioactivity studies of the schiff base ligand and its Zinc(II) complex. ARO Sci. J. Koya Univ. 2024;12(1):108–114. <http://dx.doi.org/10.14500/aro.11486>.
13. Shaygan S, Pasdar H, Foroughifar N, Davallo M, Motiee F. Cobalt (II) complexes with schiff base ligands derived from terephthalaldehyde and ortho-substituted anilines: Synthesis, Characterization and Antibacterial Activity. Appl Sci. 2018;8(3):385–398. <https://doi.org/10.3390/app8030385>.
14. Ceramella J, Iacopetta D, Catalano A, Cirillo F, Lappano R, Sinicropi MS. A review on the antimicrobial activity of schiff bases: Data collection and recent studies. Antibiotics (Basel) 2022;11(2):191–207. <https://doi.org/10.3390/antibiotics11020191>.
15. Domenico I, Jessica C, Alessia C, Annaluisa M, Federica G, Carmela S, *et al.* Metal complexes with schiff bases as antimicrobials and catalysts, Inorganics J. 2023;11(8):320–232. <https://doi.org/10.3390/inorganics11080320>.
16. Bahaa AA, Othman EA, Karem LK. Synthesis, characterization, and biological studies of new complexes derived from 2-(1H-benzimidazol-2-yl) aniline. IJDD. 2021;11(3):937–941.
17. Abdulrazzaq AG, Al-Hamdani AAS. Cr (III), Fe (III), Co (II) and Cu(II)Metal ions complexes with azo compound derived from 2-hydroxy quinolin synthesis, characterization, thermal study and antioxidant activity. IHJPAS .2023; 36(3):214–30. <https://doi.org/10.30526/36.3.3068>.
18. Maged SA, Maha AA, Jawza SA. Physico-chemical study of Mn(II), Co(II), Cu(II), Cr(III), and Pd(II) complexes with schiff-base and aminopyrimidyl derivatives and anti-cancer, antioxidant, antimicrobial applications. Molecules. 2023;28:2555. <https://doi.org/10.3390/molecules28062555>.
19. Hassan, S.S., Ibrahim, S.K., Mahmoud, M.A., Alias, M.F. Synthesis and characterization of some metal complexes with new ligand(C15H10N4O7SCL) & theoretical treatment. Systematic Sys Rev Pharm. 2020;11(12):747–753. <https://doi.org/10.5530/srp.2019.1.19>.
20. Anita Priyanka G, Kavita P. Synthesis, characterization and biological activities of novel Schiff base ligand and its Co(II) and Mn(II) complexes. Res Chem. 2024;101221. <https://doi.org/10.1016/j.rechem.2023.101221>.
21. El-Megharbel SM, Qahl SH, Ali FS, Hamza RZ. Synthesis, spectroscopic studies for five new Mg (II), Fe (III), Cu (II), Zn (II) and Se (IV) ceftriaxone antibiotic drug complexes and their possible hepatoprotective and antioxidant capacities. Antibiotics (Basel). 2022;11(5):547–559. <http://dx.doi.org/10.3390/antibiotics11050547>.
22. Racheal OA, Ikechukwu PE, Hadley SC. Schiff base metal complexes as a dual antioxidant and antimicrobial agents, J. Appl. Pharm. Sci. 2023;13(3):132–140. <https://doi.org/10.7324/JAPS.2023.91056>.

تحضير وتشخيص ودراسة الفعالية البايولوجية لمشتقات السيفيبيم مع المعادن الانتقالية ثنائية التكافؤ

زهراء عبد المهدي جابر، اسراء حمود ابراهيم، سحر صبيح حسن

قسم الكيمياء، كلية العلوم للبنات، جامعة بغداد، بغداد، العراق.

الخلاصة

تم مؤخرًا تصنيع ربيطة شيف (Z)-((7-1-(L)-، 2-5,5-(Z)- ثنائي إيثيل-2-ميثوكسي إيمينو) أسيتاميدو)-2-(-2,6-methoxycarbonyl)أوكسيتيتراهدروبيريميدين-4(1-H)يلدين أمينو) ثيازول-4-يل-8-أوكسي-5-ثيا. يُسمح للأيونات المعدنية التالية، Ni^{2+} ، Cu^{2+} ، Zn^{2+} ، و Co^{2+} ، بالتفاعل مع 1-أزابيسكلو [4.2.0]أوكت-2-إن-3-يل)ميثيل)-1-ميثيلبيروليدينيوم، مما يؤدي إلى تكوين معقدات معدنية جديدة بأشكال هندسية مميزة. من خلال الكشف عن التحول في نطاق الأزومثينات وظهور نطاقات M-N و M-O، أكدت تقنية FT-IR حدوث التنسيق من خلال N من الأزوبيزولين وذرتين O من البيتا لاكتام والإستر، مما يشير إلى تطور معقدات قاعدة شيف وكذلك قاعدة شيف الأصلية. بالإضافة إلى ذلك، يمكننا استخدام مثل هذه المعقدات لمعرفة ما إذا كانت هناك أي جزيئات ماء مائية داخل مجال التنسيق. من خلال مراقبة تحول الانتقالات الإلكترونية التي حدثت في اللكيند في منطقة الأشعة فوق البنفسجية، أظهرت طيف الأشعة فوق البنفسجية-المرئية لجميع الناتجات تكوين التنسيق. تحليل TGA للرابطة. علاوة على ذلك، كانت نتائج FAA والوصولية المولية أكثر توافقًا مع نتائج العد. أظهرت التشخيصات سلوكًا ثلاثي الأسنان، وهندسة رباعية السطوح لمركب الكوبالت، وهندسة ثمانية السطوح للمركبات المتبقية، بالإضافة إلى المركبات أحادية النواة. كما هو موضح في البحث، قمنا بتقييم الخاصية المضادة للبكتيريا لقاعدة شيف ومعقداتها على مجموعة متنوعة من الميكروبات.

الكلمات المفتاحية: السيفيبيم، قواعد شف، الباربيتون، المعقدات الفلزية، التحاليل الحرارية، الفعالية البايولوجية.